J. Biochem. 2010;147(4):601–609 doi:10.1093/jb/mvq015

JB THE JOURNAL OF BIOCHEMISTRY

Function of activation loop tyrosine phosphorylation in the mechanism of c-Kit auto-activation and its implication in sunitinib resistance

Received February 1, 2010; accepted February 3, 2010; published online February 10, 2010

Jonathan P. DiNitto[1,*,†], Gayatri D. Deshmukh[1,†], Yan Zhang[1], Suzanne L. Jacques[1], Rocco Coli[1], Joseph W. Worrall[1], Wade Diehl[2], Jessie M. English[1,‡] and Joe C. Wu[1,*]

[1]Pfizer Research Technology Center, 620 Memorial Drive, Cambridge, MA 02139 and [2]Pfizer Structural and Computational Biology, 10770 Science Center Drive San Diego CA 92121, USA

*Jonathan P. DiNitto, Pfizer Research Technology Center, 620 Memorial Drive, Cambridge, MA 02139, USA, Tel: +1 617 551 3147, Fax: +1 617 551 3178, email: jdinitto@msn.com

*Joe C. Wu. Pfizer Research Technology Center, 620 Memorial Drive, Cambridge, MA 02139, USA, Tel.: +1 617 551 3147, Fax: +1 617 551 3178, email: joecwu@msn.com

†These authors contributed equally to this work.

‡Present address: Department of Oncology, Merck Research Laboratories, 33 Avenue Louis Pasteur, Boston, MA 02115, USA

The activation of receptor tyrosine kinases (RTKs) is tightly regulated through a variety of mechanisms. Kinetic studies show that activation of c-Kit RTK occurs through an inter-molecular autophosphorylation. Phosphopeptide mapping of c-Kit reveals that 14–22 phosphates are added to each mol of wild-type (WT) c-Kit during the activation. Phosphorylation sites are found on the JM, kinase insert (KID), c-terminal domains and the activation loop (A-loop), but only the sites on the JM domain contribute to the kinase activation. The A-loop tyrosine (Y_{823}) is not phosphorylated until very late in the activation (>90% completion), indicating that the A-loop phosphorylation is not required for c-Kit activation. A sunitinib-resistant mutant D816H that accelerates auto-activation by 184-fold shows no phosphorylation on the A-loop tyrosine after full activation. A loss-of-phosphorylation mutation Y823F remains fully competent in auto-activation. Similar to WT and D816H, the unactivated Y823F mutant binds sunitinib and imatinib with high affinity ($K_D = 5.9$ nM). But unlike the WT and D816H where the activated enzymes lose the ability to bind the two drugs, activated Y823F binds the two inhibitors effectively. These observations suggest that the A-loop of activated Y823F remains flexible and can readily adopt unactivated conformations to accommodate DFG-out binders.

Keywords: A-loop/autophosphorylation/tyrosine kinase/c-Kit/sunitinib/imatinib.

Abbreviations: RTK, receptor tyrosine kinase; SCF, stem cell factor; JM, Juxtamembrane; KID, kinase insert domain.

Receptor tyrosine kinases (RTK) play a key role in a host of cellular processes including differentiation and cell growth. The kinase c-Kit is a class III RTK consisting of five IgG-like extracellular domains, a transmembrane domain followed by a cytoplasmic kinase domain. This class also includes the Platelet Derived Growth Factor (PDGF), fms-related tyrosine kinase 3 (FLT3) and the Colony Stimulating Factor (CSF-1) receptors (*1–3*). Activation of c-Kit occurs upon binding Stem Cell Factor (SCF) to the extracellular domain which leads to autophosphorylation of the cytoplasmic kinase domain and activation of downstream-signalling molecules (*4–6*).

Despite the wealth of information on the effectors and downstream-signalling events that occur upon stimulation of cells with SCF, the molecular mechanism of activation of c-Kit remains not fully elucidated. There are multiple phosphor-acceptor sites in the kinase domain, including Y_{823} on the activation loop, known to be phosphorylated on c-Kit either through autophosphorylation or by other kinases in *trans* (*1*, *7*, *8*). Activation loop tyrosine autophosphorylation is generally thought to regulate kinase activation of RTKs (*9*, *10*). However, A-loop tyrosine phosphorylation may play very different roles in regulating kinase activation, depending on the individual kinase. For example, EGFR activation loop phosphorylation has no effect on the catalytic activity of the kinase but rather provides a docking site for the SH2 domain of STAT5 (*11*, *12*). This is in contrast to the Tie2 RTK in which the A-loop tyrosine is phosphorylated early in a sequential manner in autophosphorylation reactions followed by Y_{1110}. This residue is required for downstream interactions with SH2 domains (*13*). The resulting active Tie2 has a 100-fold increase in k_{cat} and a 460-fold increase in k_{cat}/K_m compared to the unphosphorylated enzyme.

In the case of c-Kit, the specific role of the A-loop tyrosine Y_{823} in the activation process is unknown. Structural studies of c-Kit indicate that upon activation, a shift in the conformation of the Asp_{810}-Phe_{811}-Gly_{812} motif (DFG) at the N-terminus of the A-loop occurs. In the active conformation, the A-loop extends over the C terminus of the catalytic pocket and the Phe_{811} moves away from the ATP-binding region ('DFG-in'), thereby creating catalytically active conformation of the kinase. Although it is known that the shift between active and inactive conformation must be controlled by phosphorylation/dephosphorylation, the exact mechanism is not clear. Little is known about the functional role of the A-loop tyrosine plays, nor about the multiple phosphorylation sites in the JM (Juxtamembrane) and KID (Kinase Insert)

domains. In addition, the sequence of 14–22 phosphorylation events of c-Kit leading to full activation of kinase activity is poorly understood.

In H526 cells, Y_{823} is phosphorylated upon SCF stimulation (*14*). This may imply a possible functional role of A-loop phosphorylation in c-Kit activation. On the other hand, a crystal structure of active c-Kit shows Y_{823} unphosphorylated (*15*), suggesting that the phosphorylation of Y_{823} may not be required. In another crystal structure where c-Kit assumes an enzymatically unactivated conformation, Y_{823} is positioned in the kinase active site and hydrogen bonded to the catalytic base (D792) thus blocking access to the catalytic centre and maintaining the enzyme in the inhibited state (*16*). Hence phosphorylation of c-Kit Y_{823} could function to disengage the A-loop from the inhibitory state rather than to activate the enzyme. In this report, several mutants are generated to investigate the roles phosphorylated and unphosphorylated Y_{823} play in shifting the conformational equilibrium between the activated and unactivated state.

Material and Methods

Expression and purification of c-Kit wild-type (WT) and mutants

c-Kit constructs were expressed and purified as previously described (*15*). Briefly, the construct encoding an N-terminal 6× HIS tag + r3c protease site + c-Kit residues 544–976 was cloned into baculovirus vector pVL1393. High titre stock was made and expressed in Sf9 cells at multiplicity of infection of 1 for 48 h. Cells were harvested and frozen −80°C. The pellet was lysed in 25 mM Tris pH 7.4, 250 mM NaCl, 0.25 mM TCEP, 20 mM imidazole and bound to Ni–NTA column. The protein was step eluted using same buffer with 250 mM imidazole. Peak fractions were dialysed overnight at 4°C. For the WT protein, the HIS tag was cleaved with r3C protease. Protein was reloaded on Ni–NTA to remove cleaved HIS tag. Flow through was collected from column and concentrated. Samples were run on Superdex-200 column equilibrated with 25 mM Tris pH 7.4, 250 mM NaCl, 0.5 mM TCEP and 1 mM EDTA. Peak fractions were pooled, concentrated and flash frozen.

c-Kit activation and phosphopeptide mapping

The kinase domain construct of WT (1.0 μM), D816H (0.7 μM) or Y823F (1.0 μM) c-Kit (amino acids 544–976) was activated by the addition of ATP to 4 mM in buffer consisting of 50 mM Tris pH 7.6, 10 mM $MgCl_2$, 3 μM Na_3VO_4, 1 mM EGTA. Samples were incubated at room temperature for WT and Y823F or on ice for D816H. Aliquots were then removed at various time points and the activation reaction was quenched by addition of EDTA to 12 mM. Trypsin and chymotrypsin digestion of c-Kit was carried out in 50 mM NH_4HCO_3 buffer as described (*17*) with slight modifications. Samples were denatured by incubation at 95°C for 5 min. Followed by reduction with DTT (4.5 mM) at 56°C for 20 min. Denatured samples were then alkylated with iodoacetamide (10 mM) for 15 min. Trypsin, chymotrypsin and lys-C digestion were then performed by adding 1 : 10 enzyme weight/weight ratio protease and incubated overnight at 37°C for trypsin and lys-C and room temperature for chymotrypsin. LC–MS–MS analysis was performed on a Thermo-fisher LTQ mass spectrometer coupled with an Eksigent 2D nano-LC with a nano-electrospray source from New Objective™ (MA, USA). A Picofrit ProteoPep2 column (10 cm) was used. The MS–MS data were collected in positive mode using data-dependent zoom scan. Phosphorylation site search was performed using SpectrumMill and Mascot software.

Direct binding of sunitinib to c-Kit mutants

Direct sunitinib binding to unactivated mutants Y823A, Y823D and Y823F was detected by measuring intrinsic Trp fluorescence quenching that occurs upon drug binding to c-Kit as described in (*18*).

Determination of auto-activation rate constant k_{act}

Activation of c-Kit at saturating ATP concentration was monitored using ATP-regenerating system composed of 4 mM ATP, 4 mM PEP, 0.5 mM NADH, 2.5 mg/ml poly Glu-Tyr, 25 U/ml PK and 31 U/ml LDH, in Buffer A (50 mM HEPES, pH 7.5, 10 mM $MgCl_2$, 1 mM EGTA, 3 μM Na_3VO_4, 0.01% Brij-35). For a bimolecular auto-activation reaction coupled with a kinase activity assay performed at saturated substrate concentration, the integrated rate equation relating the change in ADP concentration to the auto-activation rate constant (k_{act}) is:

$$\Delta[\mathrm{ADP}]_t = [c - \mathrm{Kit}_{ua}]_0 \bullet k_{cat} \bullet t - (k_{cat}/k_{act}) \times \ln([c - \mathrm{Kit}_{ua}]_0 \bullet k_{act} \bullet t + 1) \quad (1)$$

Data from auto-activation reaction progress curves were fit the above equation to determine the k_{act} and k_{cat} as described in (*18*).

IC_{50} determinations

For IC_{50} determinations of sunitinib and imatinib against pre-activated c-Kit, 10 μl of 400 nM pre-activated c-Kit was incubated with 10 μl of 0–90 μM sunitinib or imatinib at 20°C for 30 min. This was followed by addition of 80 μl of the ATP-regenerating system as described above with the exception that 0.25 mg/ml poly Glu-Tyr substrate was used. Kinase activity was then monitored by following the linear decrease of A_{340}. In order to measure IC_{50} for the inhibition of c-Kit auto-activation, 10 μl of 400 nM unactivated c-Kit kinase was pre-incubated with 10 μl of 0–90 μM sunitinib or imatinib at 20°C for 30 min, followed by addition of 10 μl of 12 mM ATP to initiate the c-Kit auto-phosphorylation. The autophosphorylation/activation was allowed to continue for 1 h at 20°C. Reaction wells were sealed to avoid evaporation. Progress of the auto-activation reaction was followed by determining the resultant active c-Kit activity by the addition of 70 μl of ATP-regenerating coupled assay

mixture. Eleven-point dose response curves with inhibitor concentration ranging from 0.3 nM to 30 μM were used to determine IC_{50}.

Steady-state determination of K_m, V_{max}

Kinetics experiments to determine V_{max} and K_m for ATP were preformed using pre-activated c-Kit prepared by incubating 10-μM unactivated enzyme with 4 mM ATP in Buffer A for 3 h at room temperature. Free ADP/ATP was removed prior to performing experiments by running samples through two sequential Sephadex G-50 columns (Sigma) bed volume 3 ml. The activated enzyme was then stored at −80°C for future uses. c-Kit kinase activity was determined using an ATP-regenerating system as described above. The steady-state rate of poly Glu-Tyr phosphorylation was calculated from the observed linear decrease of A_{340} due to the coupled oxidation of NADH, using 6,220 as the molar absorbance of NADH. In the absence of phosphor-acceptor poly Glu-Tyr, NADH depletion was negligible. To assure that our derived V_{max} parameters reflected concentrations of active enzyme, active enzyme concentration was determined by active site titration as described (*19*, *20*).

Measurement of IC50 as a function of activation time

WT c-Kit (0.5 μM) in buffer consisting of 50 mM Tris pH 7.6, 10 mM $MgCl_2$, 3 μM Na_3VO_4, 1 mM EGTA was auto-activated by the addition of 4 mM ATP. Activation reaction was stopped by the addition of EDTA to 12 mM. The IC_{50} for sunitinib was then measured in Buffer A as described above using 10 nM c-Kit.

Results

Auto-activation and phosphopeptide mapping

In order to study the sequence of phosphorylation events that lead up to c-Kit activation, phosphorylation sites and kinase activity were monitored closely during an activation reaction. As shown in Fig. 1, under the indicated experimental conditions, maximal kinase activity of WT c-Kit was obtained within 3 h. The phosphorylation of c-Kit in this auto-activation reaction yielded multiple phosphorylated species with 0–1 phosphate per c-Kit molecule before the reaction, and 14–22 phosphates on each c-Kit after full activation (Fig. 1A and B). Throughout the course of activation, aliquots of the reaction mixture were collected and analysed in phosphopeptide mapping experiments as well as in a kinase activity assay. The results are summarized in Table I. Mass spectra of intact c-Kit prior to trypsin and chymotrypsin digestion show 14–22 phosphates incorporated after full activation, however phosphopeptide mapping experiments revealed 9, 8 and 11 phosphates in the fully activated kinase for WT, D816H and Y823F mutants, respectively. This is most likely due to the presence of phosphopeptide species not detectable as a result of poor ionization efficiencies and/or low abundance of phosphopeptide resulting from the protease digestion.

In the course of WT c-Kit auto-activation, phosphorylation first takes place in the JM domain

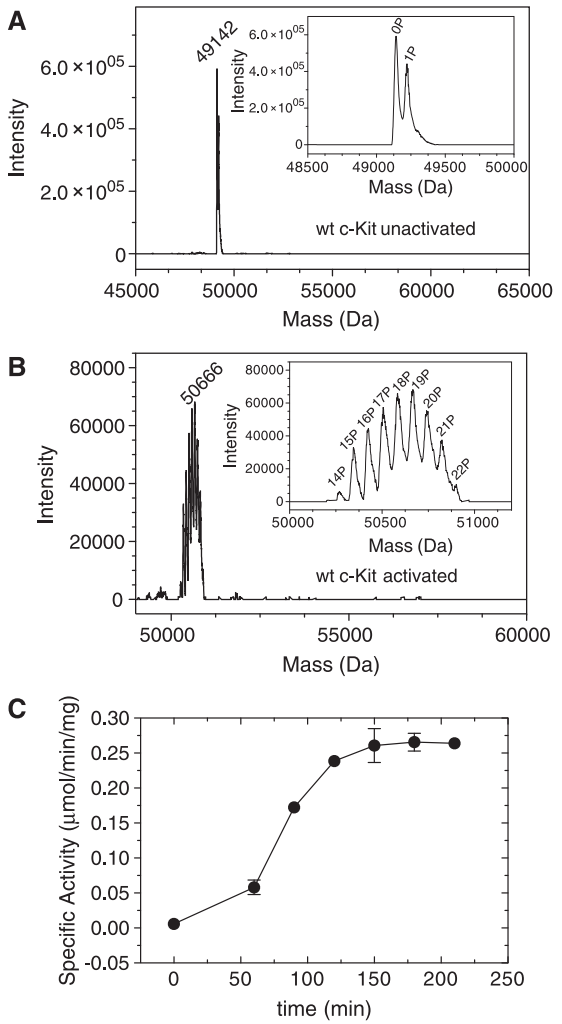

Fig. 1 LC–MS spectra of intact WT c-Kit. (**A**) Mass spectra of unactivated c-Kit WT prior to incubation ATP. (**B**) Mass spectra for fully phosphorylated activated form following incubation with 4 mM ATP for 3 h at 10-μM c-Kit concentration. (**C**) Specific activity of c-Kit vs time for samples analyzed by Mass spectrometry. Auto-activation reaction was carried out at 1-μM c-Kit with 4 mM ATP for a time course of 3.5 h.

on tyrosine residues Y547, Y553, Y568 and Y570. Phosphorylation at these positions accounts for 85% of what's needed for full activation. The activation loop tyrosine Y_{823} is subsequently phosphorylated, but does not further contribute to activation. In addition to these two phosphorylation events, multiple residues in the KID are phosphorylated as well, including S729 and/or Y730, Y703 and Y721. Assignment of pS729 and pY730 was not possible for WT and D816H c-Kit since there was insufficient MS–MS fragmentation data for this peptide in either trypsin or chymotrypsin digestions. It is not clear whether phosphorylation in KID contributes to kinase activation as it takes place concurrently with the phosphorylation in JM domain. pY703 and pY721 in KID have been postulated to be responsible for relaying signals to downstream effector proteins such as Grb2 (*21*) and Csk homologous kinase (*22*) in the process of signal transduction.

Table I. Phosphopeptide mapping of WT, D816H and Y823F c-Kit.

Time (min)	% activity	specific activity (μmol/min/mg)	Phosphorylation sites
			Wild Type
0	0	0.006 ± 0.004	
60	20	0.058 ± 0.010	*Y547, Y553,* Y703, Y721
90	64	0.172 ± 0.008	*Y547, Y553, Y568,* Y703, Y721, (S729/Y730), S959
120	90	0.239 ± 0.007	*Y547, Y553, Y568, Y570,* Y703, Y721, (S729/Y730), S959
150	99	0.261 ± 0.024	*Y547, Y553, Y568, Y570,* Y703, Y721, (S729/Y730), **Y823**, S959
180	100	0.265 ± 0.013	*Y547, Y553, Y568, Y570,* Y703, Y721, (S729/Y730), **Y823,** S959
210	100	0.264 ± 0.007	*Y547, Y553, Y568, Y570,* Y703, Y721, (S729/Y730),**Y823,** S959
			D816H
0	0	0.007 ± 0.012	
1	20	0.041 ± 0.014	*Y568,* Y703, Y721, S959
2	31	0.060 ± 0.023	*Y547, Y553, Y568, Y570,* Y703, Y721, (S729/Y730), S959
4	50	0.090 ± 0.015	*Y547, Y553, Y568, Y570,* Y703, Y721, (S729/Y730), S959
6	90	0.156 ± 0.021	*Y547, Y553, Y568, Y570,* Y703, Y721, (S729/Y730), S959
8	93	0.161 ± 0.036	*Y547, Y553, Y568, Y570,* Y703, Y721, (S729/Y730), S959
10	100	0.172 ± 0.024	*Y547, Y553, Y568, Y570,* Y703, Y721, (S729/Y730), S959
			Y823F
0	0	0.008 ± 0.005	S943
4	6	0.020 ± 0.003	Y703, Y721, S943
10	7	0.021 ± 0.008	*Y547, Y568,* Y703, Y721, S729, S943
20	22	0.051 ± 0.031	*Y547, Y553, Y568,* Y703, Y721, S729,Y747, S943
40	60	0.125 ± 0.006	*Y547, Y553, Y568, Y570,* Y703, Y721, S729, Y747, S943
60	96	0.194 ± 0.041	*Y547, Y553, Y568, Y570,* Y703, Y721, S729, Y747, S943
120	100	0.203 ± 0.002	*Y547, Y553, Y568, Y570,* Y703, Y721, S729, Y747, Y900, S937, S943

JM domain are depicted in italic; KID domain are depicted by underline; activation loop are depicted by bold; C-terminal domain are in the normal font; unable to distinguish between either of these two phosphorylation sites are included in the parenthesis.

The same experiment was performed for a sunitinib resistant mutant of c-Kit, D816H. Recent studies indicated that the A-loop mutant D816H is activated 184-fold faster than WT c-Kit and the increased rate of auto-activation leads to resistance to sunitinib in patients with Gastrointestinal Stromal Tumors (*18*). As shown in Table I, phosphorylation of D816H follows exactly the same path as WT c-Kit albeit on a much shorter timescale. Under similar conditions (0.7 μM c-Kit with 4 mM ATP) full activation was observed after only 6 min at 4°C, compared to 3 h for the WT enzyme at 25°C. The second order rate constant for auto-activation (k_{act}) was reported to be 0.25 and 46 $mM^{-1}s^{-1}$ for WT and D816H, respectively (*18*). After full activity was reached, the same phosphorylation sites are found in D816H and WT, with the exception of Y_{823} in D816H. This residue was phosphorylated only after extended incubation with 4 mM ATP. Thus, phosphorylation of Y_{823} is not required for the activation of D816H, and is likely not needed for WT c-Kit as well.

Activation loop phosphorylation is a common mechanism of controlling kinase activation. Y_{823} is the only potential tyrosine phosphorylation site on the A-loop of c-Kit. If a phosphorylated Y_{823} is not required for activation, what role does the A-loop play in c-Kit, and what is the significance of Y_{823}? To address these questions, Y823F, Y823A and Y823D were expressed and purified for further studies. While no detectable kinase activity was observed for Y823A and Y823D after extended activation with ATP, Y823F mutant can be promptly activated to a similar specific activity as WT and D816H. The binding studies in Fig. 2 indicate Y823D and Y823F bind sunitinib with similar affinity as WT (*18*). This result suggests that the conformation of these variants remain unaffected, particularly in the area responsible for binding sunitinib. However the mutation Y823A most likely leads to misfolded enzyme as it is unable to bind sunitinib. Phosphopeptide-mapping experiments indicate that phosphorylation of Y823F follows the same path as WT and D816H, with virtually all identical residues phosphorylated (Table I). These results suggest that Y823F substitution does not alter the sequence of phosphorylation on other residues that lead to activation of c-Kit. However, given that Y823D is enzymatically impaired and cannot undergo auto-activation, and that Y823F is activated at a much accelerated rate compared to WT c-Kit, it seems that an appropriate side chain at this position such as Tyr or Phe is necessary for c-Kit activity and that substitution of Y823 with a negatively charged residue does not mimic phosphorylated Y823 in the context studied here.

As shown in Table I, after a 1 h activation reaction for Y823F, full activation is achieved and no increase in kinase activity is seen with extended incubation with ATP. However, phosphorylation at the KID (Y747) and the C-terminal domain (Y900, S937 and S943) continues. This may suggest that the phosphorylation of the KID in Y823F mutant contributes very little to the kinase activation. Despite having the same final phosphorylated state and similar enzymatic activity as WT enzyme, mutant Y823F and the sunitinib resistant variant D816H auto-activate much faster than WT c-Kit.

Quantitative determination of the rate of auto-activation and catalytic efficiency of activated

c-Kit was performed in an integrated assay system that couples active c-Kit production with a c-Kit catalysed poly(Glu-Tyr) phosphorylation. Fig. 3 shows representative progression curves of Y823F and WT c-Kit in this assay wherein the activation of c-Kit leads to continuous increase in kinase activity. This results in exponential accumulation of kinase reaction product ADP. Experiments performed at several concentrations of WT and Y823F variant provide data to fit to equation 1 in the 'Materials and Methods' section and afford determination of the activation and catalytic rate constants, k_{act} and k_{cat}, respectively. Accordingly, a k_{act} of $0.7\,mM^{-1}s^{-1}$ and a k_{cat} of $2.8\,s^{-1}$ for Y823F were obtained compared to a k_{act} of $0.04\,mM^{-1}s^{-1}$ and a k_{cat} of $3.6\,s^{-1}$ for WT (Table II). These results indicate that activated Y823F has a similar kinase activity as WT, but the auto-activation proceeds at a 18-fold faster rate than WT.

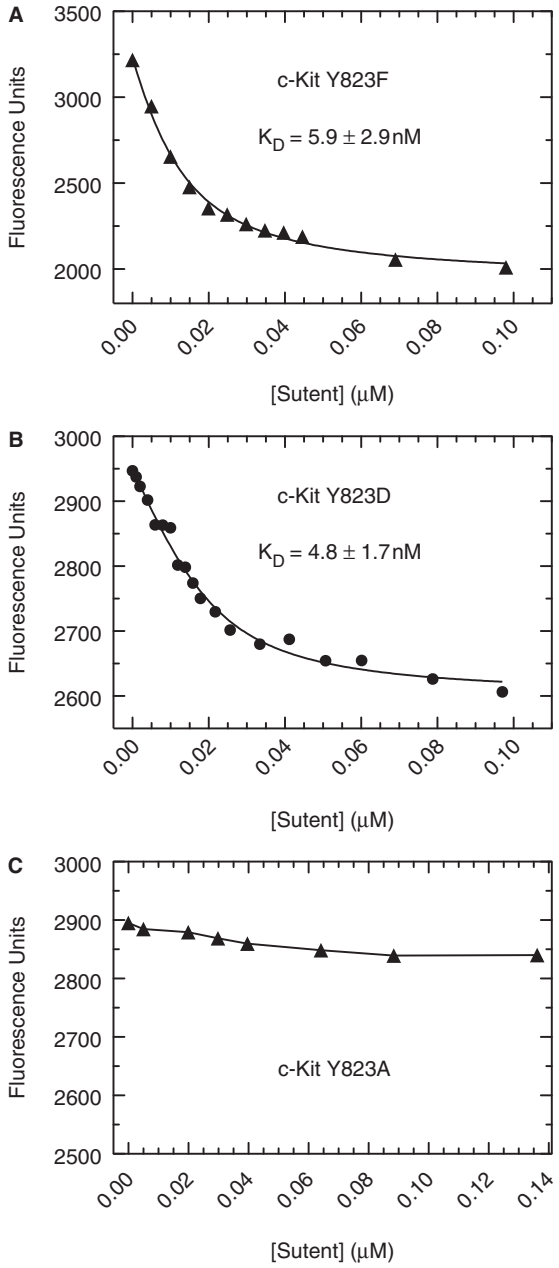

Fig. 2 Binding of sunitinib to unactivated Y823F, Y823D and Y823A. The change in intrinsic Trp fluorescence that occurs upon the interaction with sunitinib was used to monitor the binding of sunitinib to unactivated mutant forms of c-Kit. Samples of unactivated enzyme (100 nM) in kinase activity assay buffer were titrated with sunitinib. The decrease in fluorescence that occurs upon sunitinib binding was monitored using PTI fluorimeter with excitation and emission wavelengths of 293 and 340 nm respectively. Binding curves were fit to the Morrison equation as described in (*18*) yielding K_D values of 5.9 and 4.8 nM for Y823F (Panel A) and Y823D (Panel B) mutants. These values are within 3- to 4-fold those reported for the WT kinase (*18*). No detectable change in fluorescence is observed with Y823A (Panel C) variant by titration of up to 200 nM of the drug.

Inhibitor sensitivity of WT and mutants

The clinically observed mutation D816H confers resistance to sunitinib. Enzymological and structural studies demonstrate that the drug resistance is a result of the greatly increased rate of auto-activation of the mutant that leads to a rapid loss of molecules in the preferred unactivated conformation for binding sunitinib. Thus, sunitinib may be used to probe the equilibrium dynamic between activated and unactivated conformations of Y823F in phosphorylated or unphosphorylated states. As demonstrated in Fig. 4A, sunitinib prefers unactivated c-Kit conformation and is a more potent inhibitor of unactivated WT c-Kit than fully activated, phosphorylated enzyme. IC_{50} values were determined to be >20 μM and 68 nM for activated and unactivated c-Kit, respectively. The same experiment was performed using Y823F shown in Fig. 4B. Unlike WT c-Kit, fully activated Y823F is much more sensitive to sunitinib with an $IC_{50} = 200$ nM, whereas the unactivated form of the enzyme remains similar to WT c-Kit, giving an $IC_{50} = 27$ nM. Thus, the affinity for sunitinib binding to activated and unactivated

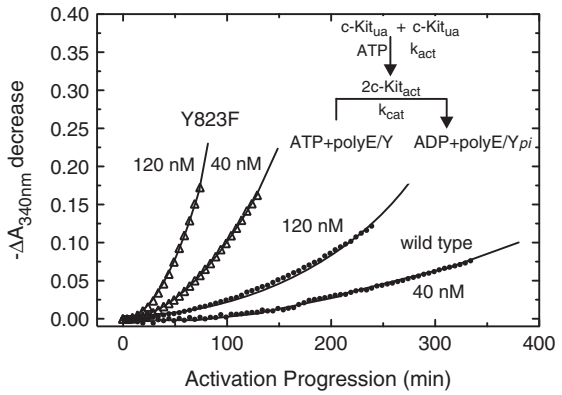

Fig. 3 Auto-activation progress curves for WT and Y823F c-Kit. Unactivated c-Kit (WT and Y823F) was incubated with ATP in the presence of 10 mM $MgCl_2$ to initiate auto-activation reaction. The readout of activated enzyme is from the phosphorylation of poly Glu-Tyr in an ATP regeneration system as described in the 'Materials and Methods' section. Fitting of the curves to Equation (*1*) gives auto-activation rates (k_{act}) of 0.04 and $0.7\,mM^{-1}s^{-1}$ for WT and Y823F mutants respectively. (*inset*) Reaction scheme for the activation of c-Kit by auto-phosphorylation. Once activated, c-Kit$_{act}$ catalyses the phosphorylation of poly Glu-Tyr substrate in NADH coupled reaction system. Once sample is completely activated, a linear reaction progress curve is observed with poly Glu-Tyr as a substrate.

Table II. Auto-activation rates, kinase activity and IC_{50} values for WT, Y823F and ΔJMΔKID-c-Kit.

	WT	Y823F	ΔJMΔKID
	Auto-activation		
k_{act} ($mM^{-1} s^{-1}$)	0.04 ± 0.002	0.7 ± 0.1	>150
k_{cat} (s^{-1})	3.6 ± 0.2	2.8 ± 1.2	–
	Steady-State Kinase Activity		
K_m (10^{-6} M)	115.0 ± 46.1	273.5 ± 160	91.5 ± 26.1
V_{max} (10^{-8} M s^{-1})	2.46 ± 0.54	1.86 ± 0.12	3.50 ± 1.55
	IC_{50} activated (μM)		
sunitinib	20.5 ± 0.7	0.200 ± 0.090	>30
imatinib	2.0 ± 1.4	0.051 ± 0.022	>30
	IC_{50} unactivated (μM)		
sunitinib	0.068 ± 0.020	0.027 ± 0.018	0.033 ± 0.025
imatinib	0.046 ± 0.005	0.093 ± 0.025	0.010 ± 0.001

Y823F only differs by 7-fold, in comparison to >300-fold for WT c-Kit. Similar results were obtained using imatinib as the probe (Table II). Imatinib is known to prefer unactivated conformation of the kinase. As such, Y823F seems to be more accommodating than the WT enzyme in shifting the equilibrium dynamic between activated and unactivated conformations, such that when sunitinib is present, fully activated Y823F can quickly adopt the unactivated conformation preferred by sunitinib binding. The increased dynamic in conformation does not affect ATP binding or kinase catalysis. As shown in Fig. 4C, ATP K_m and V_{max} of Y823F remain very similar to that of WT c-Kit.

Previous biochemical and structural studies show that the JM domain plays a critical role in the activation of c-Kit (*15*, *16*, *18*, *23*). Phosphopeptide mapping data presented in this study indicate that the initial phosphorylation occurs on four tyrosine residues on the JM domain and that the specific activity of the enzyme can be largely attributed to phosphorylation of these residues. Thus, the JM domain seems to function as a built-in inhibitor of the enzyme, and phosphorylation of the domain moves it away from the auto-inhibitory position. Is releasing the JM domain from the auto-inhibitory position sufficient to activate c-Kit? As shown in Table II, a c-Kit construct with the JM and KID domains deleted is indeed activated almost instantly upon exposing to ATP ($k_{act} > 150\ mM^{-1}s^{-1}$), consistent with the previously observed instantaneous activation of an oncogenic JM mutant V560D (*18*). The ΔJMΔKID-c-Kit was also tested against sunitinib and imatinib. Like D816H, the activated ΔJMΔKID-c-Kit is insensitive to the two DFG-out inhibitors ($IC_{50} > 30\ \mu M$, Table II). But unlike D816H where the drug sensitivity quickly diminishes during auto-activation, unactivated ΔJMΔKID-c-Kit remains sensitive to the drugs (Table II). This sensitivity is maintained throughout the 16-h course of the auto-activation reaction giving $IC_{50} = 540$ and 5 nM for sunitinib and imatinib after 16 h, respectively (*18*). Therefore, removal of JM domain does not significantly affect the A-loop such that ΔJMΔKID-c-Kit maintains its ability to bind the

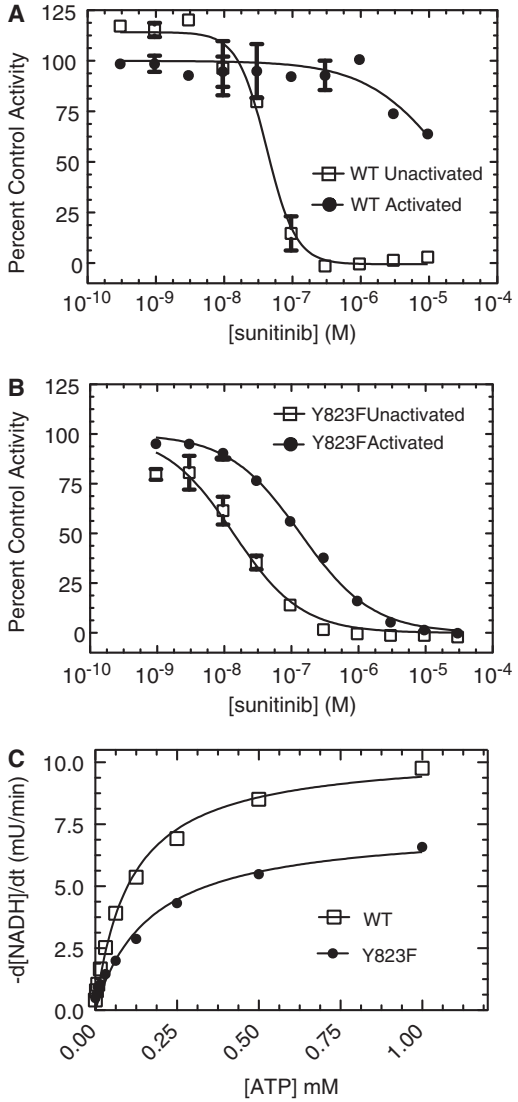

Fig. 4 Kinetic parameters and IC_{50} values for c-Kit WT and Y823F. IC_{50} curves for WT (A) and Y823F (B) c-Kit. For activated form, samples of c-Kit were pre-incubated with saturating ATP prior to IC_{50} assay as described in the 'Materials and Methods' section. (C) Kinetics for WT and A-loop mutant Y823F. ATP serially diluted 2-fold from 1 mM. Twelve point saturation curves fit to Michaelis–Menton equation yielding K_m and V_{max} values of 115.0 μM and 2.46×10^{-8} M s^{-1} for WT and 273.5 μM and 1.86×10^{-8} M s^{-1} for Y823F. *V*max values derived from fitting were determined using the active enzyme concentration measured by titration with tight binding inhibitor sunitinib as described in the Material and Methods section.

two DFG-out inhibitors in an unactivated conformation. These results suggest that the activation process requires at least two transitional domain movements: Release of JM domain from its auto-inhibitory position followed by the A-loop transitioning to the DGF-in state. Removal of the JM domain alone does not automatically convert the kinase from the unactivated to activated state.

Taken together, results from the phosphopeptide mapping and IC_{50} determinations suggest that for WT c-Kit, the sensitivity to sunitinib should be maintained if the A-loop is unphosphorylated. Y823 phosphorylation occurs late in the auto-activation, as such it should be possible to capture the kinase in a state

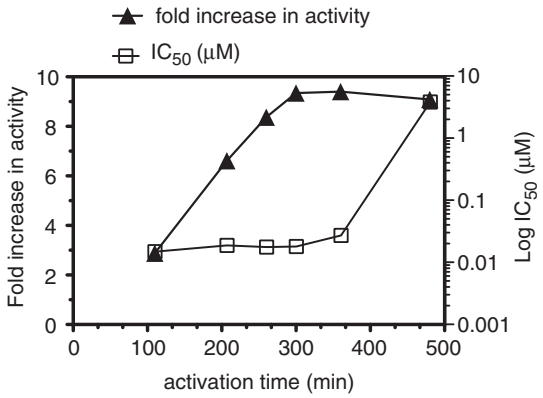

Fig. 5 IC_{50} as a function of auto-activation time for WT c-Kit. WT c-Kit (0.5 μM) was activated by addition of 4 mM ATP in the presence of 10 mM $MgCl_2$. Reaction was then quenched by the addition of 12 mM EDTA. Samples were then diluted to 10 nM in buffer A and the IC_{50} for sunitinib was measured. Activity of c-Kit reaches a maximum at 300 min while the course of IC_{50} increases at a slower rate, reflecting the slow phosphorylation of Y823 in the auto-activation process. Under these conditions, intermediate phosphorylated forms of c-Kit in which Y823 is unphosphorylated are the predominant species from 0–360 min auto-activation time.

that is active yet still remains sensitive to sunitinib. To examine this, we measured the IC_{50} as a function of auto-activation time. As shown in Fig. 5, the overlay of IC_{50} and the relative activity show the curves are not superimposable. Under the conditions tested, at 300 min, the kinase has reached full activity yet the IC_{50} is 37 nM. Only after extended activation time of 480 min does the IC_{50} reach the upper limit of detection of 30 μM. Thus, simply reaching full activity by autophosphorylation of tyrosine residues in the JM domain does not correlate with insenstivity to sunitinib, but rather A-loop phosphorylation is the major determinant that locks the conformation of c-Kit into a state that is not compatible with high affinity binding of sunitinib.

Discussion

It has been observed that there are multiple phosphorylation sites in the JM, KID and C-terminal domains c-Kit (*7*, *21*, *22*, *24–27*). In addition to those responsible for kinase activation in the JM domain, several phosphorylated residues have been implicated in the recruitment of downstream effector proteins in both the JM and KID domains, e.g. pY568 for the adaptor protein Lnk (*28*) and pY703/pY721 for Grb2 and PI 3-kinase respectively (*2*)· Deletion of the KID results in decreased in SCF-stimulated PI-3 kinase activity in T18 and COS-1 cells (*26*, *29*). Data presented here indicate that the activation process of c-Kit occurs sequentially with respect to the JM and activation loop tyrosine phosphorylation. In addition to these sites, the autophosphorylation reaction leads to the presence of phospho-serine sites (S729, S937, S943 and S959), these most likely are due to non-specific activities as no other reports indicate c-Kit is a dual specificity kinase in cells. In addition, the data reported here have been determined utilizing the soluble cytoplasmic kinase domain which may alleviate constraints on kinase specificity imposed by membrane proximal regions in the context of the full length receptor. The earliest detected phosphorylation sites in all three variants are located on the KID domain (Y703 and Y721) as shown in Table I. Phosphorylation of the KID domain is unlikely to be required for activation since KID truncated c-Kit retains full kinase activity (data not shown). Residues on the KID are essential for binding downstream effectors [reviewed in (*1*, *2*)], thus initial phosphorylation of the KID would facilitate the rapid transduction of signals in response to SCF stimulation.

Phosphopeptide mapping results presented here are in contrast to the autophosphorylation of fibroblast growth factor receptor 1 (FGFR1) receptor kinase domain, in which initial autophosphorylation of a A-loop tyrosine (Y_{653}) leads to 50- to 100-fold increase in catalytic activity followed by phosphorylation of residues involved in binding signalling molecules (*30*, *31*). Further 10-fold activation is achieved by phosphorylation of a second tyrosine in the A-loop (Y_{654}) in the last step of auto-activation. These differences reflect diverse mechanisms of controlling activation of the cytoplasmic kinase domain. c-Kit is maintained in the unactivated state primarily through auto-inhibition by the JM domain blocking the catalytic site in addition to the A-loop tyrosine interacting with the catalytic aspartate (D_{792}) whereas FGFR is auto-inhibited by a conserved proline (P_{663}) and residues N-terminal which are situated to obstruct the protein substrates-binding site [reviewed in (*32*)]. Full activation of FGFR1 kinase domain requires phosphorylation of two adjacent A-loop tyrosine residues, Y_{653} and Y_{654} (*33*).

Both Y823F and D816H variants of c-Kit are auto-activated much faster than WT. While the mechanism is not completely clear, it is possible that the two substitutions result in a subtle conformational change that doesn't involve the sunitinib-binding site however it renders unactivated c-Kit more susceptible to auto-activation. After activation, although the two mutants are almost indistinguishable from WT with respect to their kinase activity, they respond very differently to inhibitors that prefer a DFG-out conformation such as sunitinib and imatinib. Active WT and D816H lose their sensitivity to sunitinib completely ($IC_{50} > 20{,}000$ nM), whereas Y823F remains very sensitive to the drug ($IC_{50} = 200$ nM). Such a difference may reflect the flexibility of activated enzyme in adopting an unactivated conformation. In the activated state, despite being phosphorylated on the same residues, Y823F and WT may be very different in their conformational dynamic such that Y823F can readily adopt the DFG-out conformation and bind sunitinib or imatinib, whereas WT and D816H can not. Thus, mutation of Y_{823} to F does not prevent the enzyme from activation, but it leads to a more accommodating c-Kit that remains sensitive to the drugs after activation. Accordingly, pY_{823} in WT is likely to be responsible for stabilizing or 'locking' the A-loop at the active position.

Is Y_{823} of any significance in the unactivated state of c-Kit? Since mutant Y823F can be activated

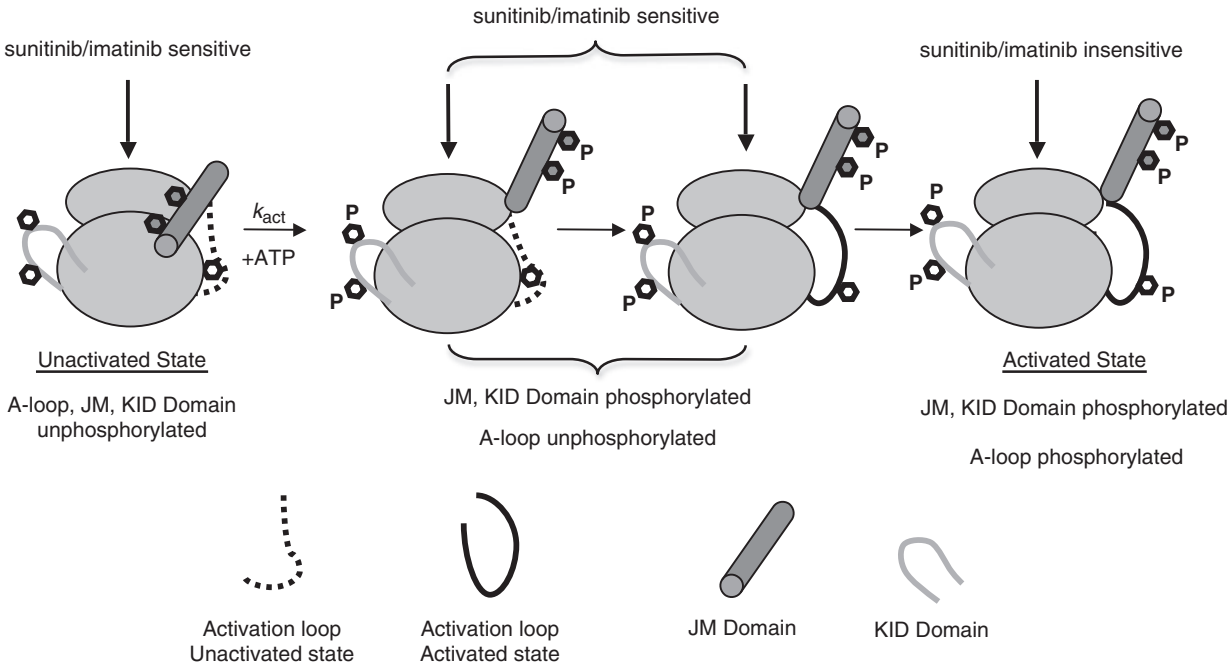

Fig. 6 Model for the activation of WT c-Kit kinase domain. Initial phosphorylation of tyrosine residues Y547, Y553, Y568, Y570 in the JM domain result in activation of the kinase. However, the activated kinase in this phosphorylation state lacking Y823 phosphorylation remains sensitive to sunitinib as the A-loop remains flexible. A much slower phosphorylation on Y823 occurs and this leads to decreased flexibility and insensitivity to DFG-out specific compounds sunitinib and imatinib. When Y823 is mutated to Phe, the last step cannot occur and the kinase remains sensitive to sunitinib. Mutation of Y823 to Asp is not an effective mimic of the phosphorylated state as this kinase unactivatable.

successfully, it seems reasonable to expect the same activation with a variety of mutations at this position. Surprisingly, Y823D renders the enzyme unactivatable although fully competent to bind sunitinib. This result suggests that an appropriate side chain at this position is necessary for unactivated c-Kit to maintain a conformation susceptible to auto-activation. In the physiological context, Y823 phosphorylation may be critical for stabilizing the activated state and preventing it from reverting back to the unactive form. As such, pY823 may be an important determinant for relaying downstream signalling events that require the kinase to be 'locked' in the activated state. The effects of the Y823F mutation on the c-Kit-signalling pathway are the subject of further studies.

Taking into account the observations presented in this study, we propose a model for the activation of c-Kit shown in Fig. 6. In this model, there are two critical determinants for maintaining the unactivated state. First, the JM domain inhibits enzyme activity in *cis* by blocking access to the catalytic site and second, the activation loop is stabilized by the aromatic side chain of tyrosine or phenylalanine. These two mechanisms maintain the enzyme in an auto-inhibited or unactivated state. Upon activation, the JM domain is rapidly phosphorylated on tyrosine residues 547, 553, 568 and 570, thus releasing it from its auto-inhibitory position between the N- and C-terminal lobes. The resulting phosphorylated kinase remains sensitive to the inhibitors sunitinib and imatinib that bind to the DFG-out unactivated conformation as the A-loop is unphosphorylated. With longer activation time, phosphorylation of the A-loop tyrosine 823 occurs, resulting in decreased flexibility of the activation loop which is then locked into the active conformation. The ensemble of conformational states is shifted in going from Y_{823} to pY_{823} forms. Mutations in the activation loop may result in either a gain (Y823F) or loss (D816H) of sensitivity to inhibitors that prefer unactivated conformation such as imatinib and sunitinib.

Acknowledgements

We thank Dr Elizabeth A. Lunney for helpful discussion.

Conflict of interest
None declared.

References

1. Roskoski, R. Jr. (2005) Structure and regulation of Kit protein-tyrosine kinase – the stem cell factor receptor, *Biochem. Biophys. Res. Commun.* **338**, 1307–1315
2. Roskoski, R. Jr. (2005) Signaling by Kit protein-tyrosine kinase – the stem cell factor receptor, *Biochem. Biophys. Res. Commun.* **337**, 1–13
3. Yarden, Y., Kuang, W.J., Yang-Feng, T., Coussens, L., Munemitsu, S., Dull, T.J., Chen, E., Schlessinger, J., Francke, U., and Ullrich, A. (1987) Human proto-oncogene c-kit: a new cell surface receptor tyrosine kinase for an unidentified ligand. *EMBO J.* **6**, 3341–3351
4. Herbst, R., Shearman, M.S., Jallal, B., Schlessinger, J., and Ullrich, A. (1995) Formation of signal transfer complexes between stem cell and platelet-derived growth factor receptors and SH2 domain proteins in vitro. *Biochemistry* **34**, 5971–5979
5. Lemmon, M.A., Pinchasi, D., Zhou, M., Lax, I., and Schlessinger, J. (1997) Kit receptor dimerization is

driven by bivalent binding of stem cell factor. *J. Biol. Chem.* **272**, 6311–6317
6. Herbst, R., Lammers, R., Schlessinger, J., and Ullrich, A. (1991) Substrate phosphorylation specificity of the human c-kit receptor tyrosine kinase. *J. Biol. Chem.* **266**, 19908–19916
7. Blume-Jensen, P., Wernstedt, C., Heldin, C.H., and Ronnstrand, L. (1995) Identification of the major phosphorylation sites for protein kinase C in kit/stem cell factor receptor in vitro and in intact cells. *J. Biol. Chem.* **270**, 14192–14200
8. Linnekin, D. (1999) Early signaling pathways activated by c-Kit in hematopoietic cells. *Int. J. Biochem. Cell. Biol.* **31**, 1053–1074
9. Huse, M., and Kuriyan, J. (2002) The conformational plasticity of protein kinases. *Cell* **109**, 275–282
10. Johnson, L.N., Noble, M.E., and Owen, D.J. (1996) Active and inactive protein kinases: structural basis for regulation. *Cell* **85**, 149–158
11. Boerner, J.L., Demory, M.L., Silva, C., and Parsons, S.J. (2004) Phosphorylation of Y845 on the epidermal growth factor receptor mediates binding to the mitochondrial protein cytochrome c oxidase subunit II. *Mol. Cell. Biol.* **24**, 7059–7071
12. Yang, S., Park, K., Turkson, J., and Arteaga, C.L. (2008) Ligand-independent phosphorylation of Y869 (Y845) links mutant EGFR signaling to stat-mediated gene expression, *Exp. Cell Res.* **314**, 413–419
13. Murray, B.W., Padrique, E.S., Pinko, C., and McTigue, M.A. (2001) Mechanistic effects of autophosphorylation on receptor tyrosine kinase catalysis: enzymatic characterization of Tie2 and phospho-Tie2. *Biochemistry* **40**, 10243–10253
14. Maulik, G., Bharti, A., Khan, E., Broderick, R.J., Kijima, T., and Salgia, R. (2004) Modulation of c-Kit/SCF pathway leads to alterations in topoisomerase-I activity in small cell lung cancer. *J. Environ. Pathol. Toxicol. Oncol.* **23**, 237–251
15. Mol, C.D., Lim, K.B., Sridhar, V., Zou, H., Chien, E.Y., Sang, B.C., Nowakowski, J., Kassel, D.B., Cronin, C.N., and McRee, D.E. (2003) Structure of a c-kit product complex reveals the basis for kinase transactivation. *J. Biol. Chem.* **278**, 31461–31464
16. Mol, C.D., Dougan, D.R., Schneider, T.R., Skene, R.J., Kraus, M.L., Scheibe, D.N., Snell, G.P., Zou, H., Sang, B.C., and Wilson, K.P. (2004) Structural basis for the autoinhibition and STI-571 inhibition of c-Kit tyrosine kinase. *J. Biol. Chem.* **279**, 31655–31663
17. Matsudaira, P. T. (1993) *A Practical Guide to Protein and Peptide Purification for Microsequencing*. 2nd edn, Academic Press, USA.
18. Gajiwala, K.S., Wu, J.C., Christensen, J., Deshmukh, G.D., Diehl, W., DiNitto, J.P., English, J.M., Greig, M.J., He, Y.A., Jacques, S.L., Lunney, E.A., McTigue, M., Molina, D., Quenzer, T., Wells, P.A., Yu, X., Zhang, Y., Zou, A., Emmett, M.R., Marshall, A.G., Zhang, H.M., and Demetri, G.D. (2009) KIT kinase mutants show unique mechanisms of drug resistance to imatinib and sunitinib in gastrointestinal stromal tumor patients. *Proc. Natl Acad. Sci. USA* **106**, 1542–1547
19. Morrison, J.F. (1969) Kinetics of the reversible inhibition of enzyme-catalysed reactions by tight-binding inhibitors. *Biochim. Biophys. Acta* **185**, 269–286
20. Williams, J.W., and Morrison, J.F. (1979) The kinetics of reversible tight-binding inhibition. *Methods Enzymol* **63**, 437–467
21. Thommes, K., Lennartsson, J., Carlberg, M., and Ronnstrand, L. (1999) Identification of Tyr-703 and Tyr-936 as the primary association sites for Grb2 and Grb7 in the c-Kit/stem cell factor receptor. *Biochem. J.* **341(Pt 1)**, 211–216
22. Price, D.J., Rivnay, B., Fu, Y., Jiang, S., Avraham, S., and Avraham, H. (1997) Direct association of Csk homologous kinase (CHK) with the diphosphorylated site Tyr568/570 of the activated c-KIT in megakaryocytes. *J. Biol. Chem.* **272**, 5915–5920
23. Mol, C.D., Fabbro, D., and Hosfield, D.J. (2004) Structural insights into the conformational selectivity of STI-571 and related kinase inhibitors. *Curr. Opin. Drug Discov. Devel.* **7**, 639–648
24. Kozlowski, M., Larose, L., Lee, F., Le, D.M., Rottapel, R., and Siminovitch, K.A. (1998) SHP-1 binds and negatively modulates the c-Kit receptor by interaction with tyrosine 569 in the c-Kit juxtamembrane domain. *Mol. Cell. Biol.* **18**, 2089–2099
25. Lennartsson, J., Wernstedt, C., Engstrom, U., Hellman, U., and Ronnstrand, L. (2003) Identification of Tyr900 in the kinase domain of c-Kit as a Src-dependent phosphorylation site mediating interaction with c-Crk. *Exp. Cell. Res.* **288**, 110–118
26. Serve, H., Hsu, Y.C., and Besmer, P. (1994) Tyrosine residue 719 of the c-kit receptor is essential for binding of the P85 subunit of phosphatidylinositol (PI) 3-kinase and for c-kit-associated PI 3-kinase activity in COS-1 cells. *J. Biol. Chem.* **269**, 6026–6030
27. Timokhina, I., Kissel, H., Stella, G., and Besmer, P. (1998) Kit signaling through PI 3-kinase and Src kinase pathways: an essential role for Rac1 and JNK activation in mast cell proliferation. *EMBO J.* **17**, 6250–6262
28. Gueller, S., Gery, S., Nowak, V., Liu, L., Serve, H., and Koeffler, H.P. (2008) Adaptor protein Lnk associates with Tyr(568) in c-Kit. *Biochem. J.* **415**, 241–245
29. Lev, S., Givol, D., and Yarden, Y. (1992) Interkinase domain of kit contains the binding site for phosphatidylinositol 3′ kinase. *Proc. Natl Acad. Sci. USA* **89**, 678–682
30. Furdui, C.M., Lew, E.D., Schlessinger, J., and Anderson, K.S. (2006) Autophosphorylation of FGFR1 kinase is mediated by a sequential and precisely ordered reaction. *Mol. Cell* **21**, 711–717
31. Lew, E.D., Furdui, C.M., Anderson, K.S., and Schlessinger, J. (2009) The precise sequence of FGF receptor autophosphorylation is kinetically driven and is disrupted by oncogenic mutations. *Sci. Signaling* **2**, ra6
32. Hubbard, S.R., Mohammadi, M., and Schlessinger, J. (1998) Autoregulatory mechanisms in protein-tyrosine kinases. *J. Biol.Chem.* **20**, 11987–11990
33. Mohammadi, M., Schlessinger, J., and Hubbard, S.R. (1996) Structure of the FGF receptor tyrosine kinase domain reveals a novel autoinhibitory mechanism. *Cell* **86**, 577–587